Chemical Engineering Journal 483 (2024) 149136

Contents lists available at ScienceDirect

Chemical Engineering Journal

journal homepage: www.elsevier.com/locate/cej

Optimal capacity design of amine-based onboard CO_2 capture systems under variable marine engine loads

Juyoung Oh [a], Donghoi Kim [b,*], Simon Roussanaly [b], Rahul Anantharaman [b], Youngsub Lim [a,*]

[a] Department of Naval Architecture and Ocean Engineering, Seoul National University, 1 Gwanak-ro, Gwanak-gu, Seoul 08826, Republic of Korea
[b] SINTEF Energy Research, Trondheim, Norway

ARTICLE INFO

Keywords:
Onboard carbon capture
MEA-based CO_2 capture process
Off-design performance
Ship engine load profile
Techno-economic assessment

ABSTRACT

The International Maritime Organization has adopted a strategy aiming for net-zero greenhouse gas emissions from international shipping, prompting various mitigation technologies to comply with this strengthened strategy. Carbon capture technologies are increasingly being considered to satisfy the IMO strategy. In particular, amine-based carbon capture technologies, which are emerging as the most mature option, have been proposed for onboard application. However, the conventional design approach for onboard carbon capture systems, which assumes a fixed high engine load (75–100 %), does not reflect ship operations in a low engine load range, consequently leading to oversizing and unnecessary capital investment. This study designs five MEA-based onboard carbon capture systems with different capacities (sizes) based on the exhaust gas conditions. The study investigates the off-design performance over the entire engine load range while maintaining the capacity of the capture systems at their design values. To identify the optimal capacity of the onboard carbon capture system, the off-design performance is applied to an actual sailing profile in order to quantify the energy requirement, potential CO_2 reduction rate, and capture cost. The results show that smaller systems can reach a similar level of CO_2 reduction as other larger systems while reducing capture costs. This means that it is possible to reduce capture costs by decreasing the capture capacity while maintaining the carbon reduction potential. The small capacity capture system also achieves a more competitive CO_2 avoidance cost (236 € per tonne) compared to biofuel (304 € per tonne) for a similar CO_2 avoidance rate (59 %). Thus, this study demonstrates a new approach to the design of amine-based onboard carbon capture systems under variable engine loads and presents the potential of the decarbonization technology for shipping industry.

1. Introduction

Global warming, significantly influenced by CO_2 concentration and emissions, reached its highest level in human history in 2022. According to data from the Scripps Institution of Oceanography, the CO_2 concentration is 50 % higher than the pre-industrial level [1]. Besides, global CO_2 emissions continued to increase from 34.8 billion tonnes in 2012 to 36.6 billion tonnes in 2018. This upward trend can be partly attributed to the emissions from international shipping, which increased from 2.76 % in 2012 to 2.89 % of the global CO_2 emissions in 2018 [2]. Therefore, the Marine Environment Protection Committee (MEPC) approved the Initial International Maritime Organization (IMO) Strategy to reduce greenhouse gas (GHG) emissions from ships by at least 50 % by 2050 compared to 2008 levels [3]. To achieve this strategy, the IMO has brought into effect new mandatory measures in 2022, including the Energy Efficiency Existing Ship Index (EEXI) and the Carbon Intensity Indicator (CII) [4,5]. Recently, the MEPC has adopted the 2023 IMO GHG Strategy, a strengthened revised strategy, which sets a target of net-zero GHG emissions by or around 2050 [6].

The shipping industry is making efforts to comply with the IMO strategy by switching to zero-carbon or carbon–neutral fuels [7]. However, the transition to alternative fuels has limitations as an immediate solution because it requires a high technology readiness level (TRL) and comprehensive supporting infrastructure [8]. Moreover, alternative fuels, such as green and blue hydrogen, still need time to become cost-competitive [9]. While conventional emission reduction strategies have been implemented [7,10], these existing measures alone are insufficient to satisfy the IMO's ever-strengthening GHG strategy. Therefore, readily available reduction measures are required as interim technologies until alternative fuel solutions are established.

Carbon capture and storage (CCS) technologies, which have been

* Corresponding authors.
E-mail addresses: donghoi.kim@sintef.no (D. Kim), s98thesb@snu.ac.kr (Y. Lim).

https://doi.org/10.1016/j.cej.2024.149136
Received 11 October 2023; Received in revised form 22 January 2024; Accepted 25 January 2024
Available online 1 February 2024

Nomenclature

CAPEX	Capital expenditures
CCS	Carbon capture and storage
CII	Carbon Intensity Indicator
DCC	Direct contact cooler
EEXI	Energy Efficiency Existing Ship Index
FAME	Fatty acid methyl ester
FOPEX	Fixed operating expenditures
GHG	Greenhouse gas
GTD	General Technical Data
IMO	International Maritime Organization
KPIs	Key performance indicators
LNG	Liquefied natural gas
L/G	Liquid-to-gas
MCR	Maximum continuous rating
MDEA	Methyldiethanolamine
MEA	Monoethanolamine
MEPC	Marine Environment Protection Committee
MGO	Marine gas oil
NG	Natural gas
NOAK	N^{th}-of-a-kind
NRTL	Non-random two-liquid
OCC	Onboard carbon capture
OPEX	Operating expenditures
SFOC	Specific fuel oil consumption
SEC	Specific energy consumption
SRD	Specific reboiler duty
TCR	Total capital requirement
TDC	Total direct cost
TDCPC	Total direct cost including process contingency
TPC	Total plant cost
TEU	Twenty-foot equivalent unit
TRL	Technology readiness level
VOPEX	Variable operating expenditures
WHRU	Waste heat recovery unit

proven in land-based facilities [11], are now being considered for onboard applications to achieve the IMO strategy [5]. The MEPC has recognized the potential of onboard CCS systems in reducing GHG emissions and has discussed their reflection into IMO regulations [12]. The onboard CCS systems capture CO_2 from the exhaust gas emitted from marine engines, store the captured CO_2 onboard, and unload it at storage sites [13]. The four technologies considered for carbon capture applications are chemical absorption, adsorption, membrane separation, and cryogenic separation [14–17]. To decarbonize the shipping industry in a timely manner, many studies focus on solvent-based chemical absorption, which has the highest TRL compared to other candidates.

Luo and Wang [18] proposed a solvent-based onboard carbon capture system that uses monoethanolamine (MEA) solvent. Techno-economic assessments were performed for a cargo ship based on exhaust gas conditions emitted from four-stroke engines operating at 85 % engine load. The results showed that a 73 % carbon capture rate at a capture cost of 77.5 €/tonne CO_2 could be reached by using the existing system. The study also showed that installing an additional gas turbine could achieve a 90 % carbon capture rate at a capture cost of 163 €/tonne CO_2. Feenstra et al. [19] carried out techno-economic evaluations for onboard carbon capture systems for different engines (1280 kW and 3000 kW), solvents (monoethanolamine and piperazine), fuels (liquefied natural gas and diesel), carbon capture rates (60 % and 90 %), etc. The analyses utilized exhaust gas data for four-stroke engines at 100 % engine load. Lee et al. [20] investigated a chemical absorption process for onboard carbon capture using an activated methyldiethanolamine (aMDEA) solvent. They used exhaust gas conditions from a two-stroke low-pressure dual-fuel engine operating at 75 % engine load. Long et al. [21] conducted process simulations and economic evaluations for ship-based carbon capture systems that were designed based on data from a four-stroke engine operating at 100 % engine load. They showed improvements in the CO_2 capture rate, which was increased to 94.7 %, by varying solvent selection and process configurations. Awoyomi et al. [22] analyzed process simulations and cost evaluations for an NH_3-based onboard carbon capture system based on three different engine loads for 50 %, 75 %, and 85 % of a four-stroke engine. The capital expenditures (CAPEX) for all different engine load cases were estimated only based on 85 % engine load. The results indicated that a 90 % carbon capture rate at a captured cost of 117 $/tonne CO_2 was achieved. Ros et al. [23] conducted a techno-economic analysis of onboard carbon capture systems deployed on a semi-submersible crane vessel, the Sleipnir, powered by 12 four-stroke engines. They determined the equipment size of the onboard CCS systems based on the specific engine loads for the fictitious normalized operational ship profiles. The results presented a captured cost of 119 €/tonne CO_2 for a 72.5 % carbon capture rate.

It should be noted that most of the onboard carbon capture (OCC) systems in previous studies have typically been designed based on the fixed engine load, assumed to be between 75 % and 100 % of four-stroke engines, which are mainly used to power small ships (Table 1). However, the actual engine load varies continuously during the voyage due to various operating conditions, such as route, market price, and weather. Besides, to reduce CO_2 emissions, the IMO recommends low average main engine loads for seaborne trade ships [24]. This means that OCC systems are operated at off-design load conditions predominantly over the entire voyage, rather than constantly at a single high engine load. Thus, the conventional design approach to OCC systems can lead to over-dimensioning and unnecessary capital investment.

This study aims to design an OCC system that performs well over a wide range of engine loads while selecting a proper system capacity (size). In order to identify the optimal capacity of the OCC system, five amine-based OCC systems with different capacities are developed. The off-design performance of these systems is investigated under different engine load conditions, considering an actual load profile of the marine engine. These performance results are then quantified in terms of energy requirements, potential CO_2 reduction rates, and capture costs.

2. Concept of this study

In order to determine an OCC system with optimal capacity, this study designed amine-based OCC systems with five different capacities based on the exhaust gas conditions at the main engine loads of 50 %, 60 %, 70 %, 80 %, and 90 %. The ship's main engine was considered as the onboard emission source. Exhaust gases from auxiliaries such as generators and MGO-fired boilers were assumed to be vented without CO_2 capture. As the focus of this work was on designing the capture system under variable engine loads, the liquefaction and storage systems for the captured CO_2 were not included. Fig. 1 shows a process flow diagram of the amine-based OCC process that is the scope of this study.

Since the main engine load varies continuously during the voyage, the OCC systems were analyzed in terms of both off-design performance and cumulative performance. The off-design performance at each off-design load was evaluated while maintaining the capacity of the capture systems at their design values. The engine load profile was then used to quantify the cumulative performance for the entire voyage, evaluating energy requirements, potential CO_2 reduction rates, and capture costs for each capacity scenario.

Table 1
Previous absorption-based onboard carbon capture studies.

Reference	Design-point load	Target engine	CO_2 concentration	Exhaust gas temperature (℃)
Four-stroke engine				
Luo and Wang [18]	85 %	Wärtsilä 9L46 (Diesel)	5.69 mol%	362
Feenstra et al. [19]	100 %	Wärtsilä 8L20DF (Diesel)	4.8 mol%	325
		Wärtsilä 8L20DF (LNG)	4.8 mol%	350
		Wärtsilä 6L34DF (Diesel)	4.8 mol%	381
		Wärtsilä 6L34DF (LNG)	4.8 mol%	381
Long et al. [21]	100 %	Wärtsilä 6L34DF (Diesel)	4.8 mol%	381
Ji et al. [25]	85 %	Wärtsilä 12V50DF (Diesel)	10.02 wt%	356
Awoyomi et al. [22]	85 %	Wärtsilä 9L46DF (LNG)	7.6 wt%	362
Ros et al. [23]	60 %, 71 %	MAN 8L51/60DF (LNG)	4.47 vol%	405
Two-stroke engine				
Lee et al. [20]	75 %	WinGD 6X72DF (LNG)	4.30 wt%	205
Stec et al. [26]	75 %	MAN 6S50ME-C8.5 (HFO)	3.65 vol%	224
Einbu et al. [27]	66 %	MAN 5S40ME-C9.5-GI (Diesel)	4.8 vol%	ca. 196
		MAN 5S40ME-C9.5-GI (LNG)	3.6 vol%	ca. 200

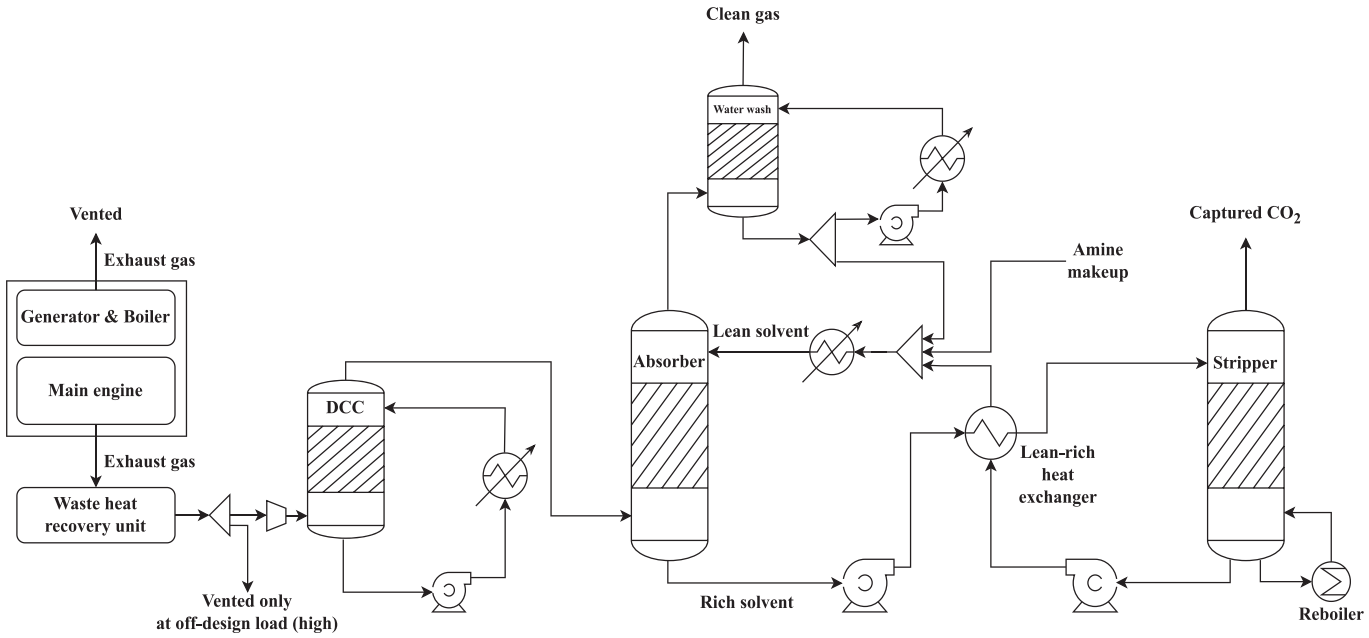

Fig. 1. Process flow diagram of the amine-based onboard carbon capture process.

3. Case study

3.1. Targeted ship

According to the results of the Third and the Fourth IMO GHG Studies, the CO_2 emissions from international shipping are dominated by three major ship types: containers, bulk carriers, and oil tankers. These ship types account for 51 % and 55 % of these emissions in 2012 and 2018, respectively [2,28]. Thus, this study considered a container ship fueled by natural gas (NG) as the target ship to have a large impact on potential CO_2 reduction in the marine industry. The main specifications of the target ship are shown in Table 2 [29].

3.2. Main engine exhaust gas conditions

For OCC systems, it is challenging to attribute a single effect to one variable, given the complexity of the capture system including the interface with ship machineries. However, the CO_2 concentration, temperature, and flow rate of the exhaust gas from a ship power system will have significant impacts on the sizing and energy consumption of onboard capture systems.

The CO_2 concentration of the exhaust gas from the main engine varies with fuel type, engine type (two-stroke or four-stroke), and engine load, typically ranging between approximately 3–6 mol% [18,20]. The main component of the energy required for CO_2 capture is the energy required to regenerate the solvent in the stripper and is referred to as specific reboiler duty – the energy required to capture 1 kg (or tonne) of CO_2. The specific reboiler duty, which consists of the desorption heat (q_{abs,co_2}), the heat required to increase the temperature of the solvent (q_{sens}), and the heat required to generate the stripping steam (q_{vap,H_2O}), is affected by the CO_2 concentration [30,31]. Thus, it is important to identify accurate CO_2 concentration in the exhaust gas with varying engine loads.

Table 2
Main specifications of the target ship [29].

Category	Unit	Value
Length over all	m	224.8
Breadth	m	37.5
Depth	m	19.1
Deadweight	DWT	53,200
Container capacity	TEU	3,840
Fuel	–	Natural gas
$MCR_{Main\ engine}$	kW	18,200 (WinGD 6X72DF)

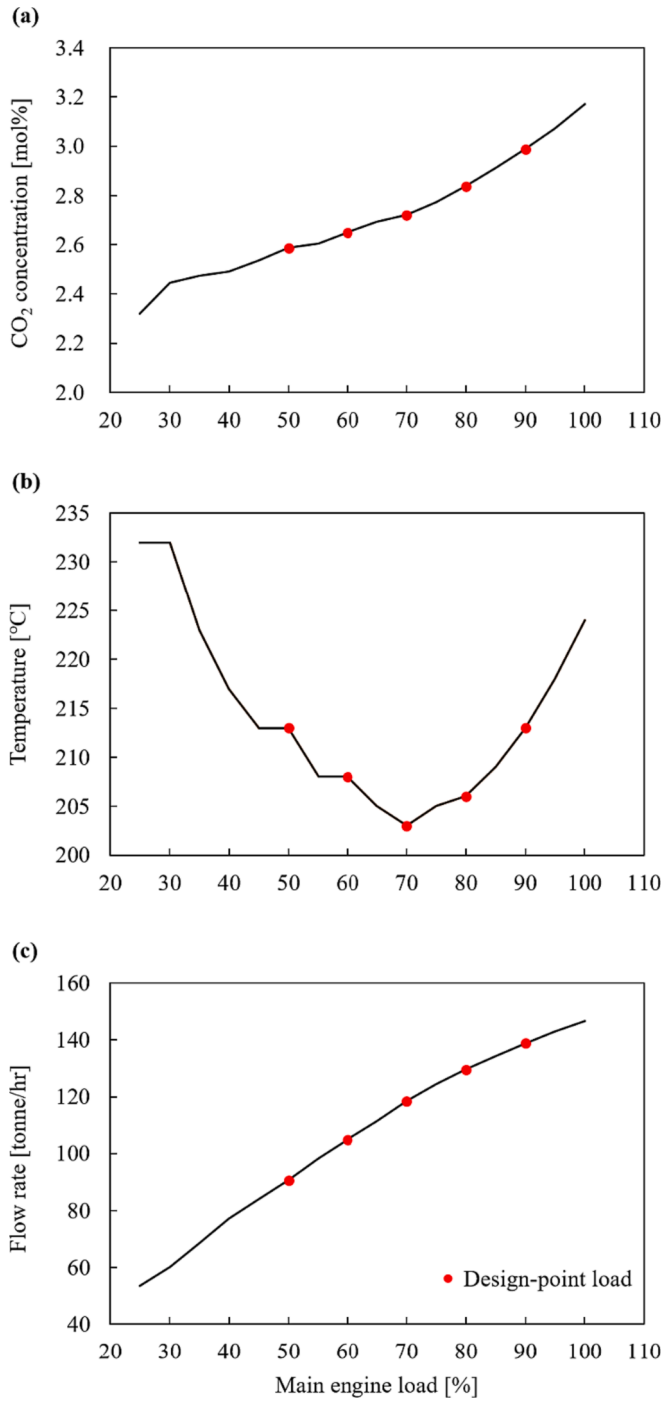

Fig. 2. Exhaust gas conditions of the main engine: (a) CO_2 concentration of the exhaust gas as function of engine load; (b) Exhaust gas temperature as function of engine load; (c) Exhaust gas flow rate as function of engine load.

The exhaust gas temperature also varies depending on the fuel type, engine type, and engine load. The temperature determines the amount of heat that can be collected from the waste heat recovery unit (WHRU), which can be utilized for the capture system. Therefore, estimating exhaust gas temperature along with different engine loads is essential to evaluate the net energy required for the onboard capture system.

Given the size of container ships has been increasing [2], a two-stroke low-pressure dual-fuel engine (WinGD X-DF), mainly used to power large ships, was selected as the main engine for this study. The exhaust gas conditions were estimated using WinGD's General Technical Data (GTD) software for the 25–100 % engine load range, the range provided by GTD. Fig. 2 shows that the two-stroke engine has a relatively low CO_2 concentration and exhaust gas temperature (avg. 2.7 mol %, 214 ℃) compared to four-stroke engines (ca. 5 mol%, 325–405 ℃). This means that additional fuel consumption is expected in the MGO-fired boiler to generate the extra heat to supply the reboiler, resulting in higher energy requirements and costs than those reported in previous studies focusing on four-stroke engines. Thus, from a carbon capture perspective, these lower conditions may be the worst assumptions for the OCC case study.

3.3. Main engine load profile

In 2018, most container fleets operated at lower engine loads than in 2012, with containers in the 3,000–4,999 TEU category operating at an average engine load of 33 % [2]. This study adopted an actual main engine load profile with a low average engine load as in the IMO study. Fig. 3 shows a main engine load profile provided by a ship operator, Klaveness Combination Carriers. The target ship operates at an average engine load of 49 %, not a high engine load.

Unlike land-based carbon capture systems in industrial facilities that typically operate at a relatively constant load, the main engine loads are not set at a specific point [23], but are varied between 36 % and 60 % load, as shown in Fig. 3. It should be noted that the marine engine is operated in the low engine load range for most of the voyage.

4. Onboard carbon capture system

4.1. Capacity scenarios

The existing design methodology for OCC systems has focused on a fixed high engine load (75–100 %). However, this approach has overlooked typical ship operations that frequently operate in low engine load ranges. In order to reflect the actual main engine load profile, five capacity scenarios were defined based on the exhaust gas conditions at engine loads of 50 %, 60 %, 70 %, 80 %, and 90 %, as shown in Table 3. Thus, in this work, five different amine-based OCC systems were designed according to their capacity scenarios. For example, in capacity scenario 1, the OCC system is designed based on the exhaust gas generated from the main engine at 50 % load, which is the design-point load of capacity scenario 1.

4.2. Process design at design-point loads

In this study, an aqueous solution of 30 wt% monoethanolamine (MEA) was selected as a solvent. Aqueous MEA solution is the most studied amine solvent for CO_2 capture [31]. The rigorous process models of the MEA-based capture process for design-point loads were developed based on the rate-based separation column model in Aspen Plus version 11 [32], which uses the unsymmetric electrolyte non-random two-liquid (NRTL) activity coefficient model for liquid properties and PC-SAFT equation of state for vapor properties. To improve the reliability of the rate-based models operating under onboard conditions, the carbon capture process model was validated against the pilot plant data reported by Notz et al. [31]. Then, the scale-up model of OCC systems was developed based on the validated model (see Appendix A). Considering the exhaust gas conditions of each design-point load (Table 3), the sizes of three main columns were determined for each capacity scenario. However, the packing height of the columns was fixed considering the limited space on the ship and the operation of marine radar. The diameter of the columns was determined based on the flooding parameter of 70 % [33], which is influenced by the lean CO_2 loading.

The lean CO_2 loading with the lowest energy consumption was investigated for each design-point load condition while maintaining the base carbon capture rate of 90 % [34,35] as shown in Fig. 4. The flow rate of the lean amine solvent was estimated based on the energy-optimal lean CO_2 loading value for the solvent. Therefore, in the

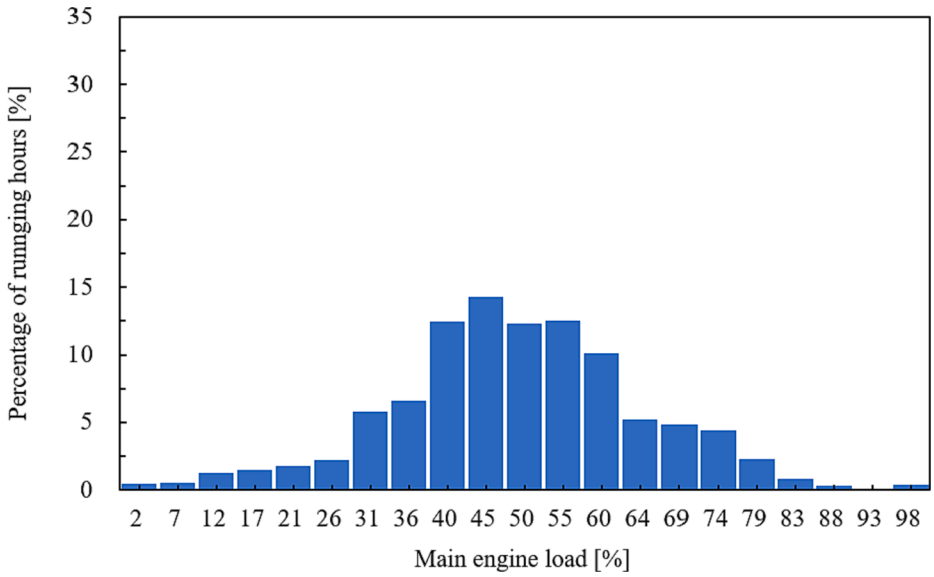

Fig. 3. Main engine load distribution of eight CLEANBU combination carriers from Klaveness Combination Carriers.

Table 3
Capacity scenarios for the design and operation of onboard carbon capture systems.

Category	Unit	Capacity scenario 1	Capacity scenario 2	Capacity scenario 3	Capacity scenario 4	Capacity scenario 5
Design-point load	%	50	60	70	80	90
Feed flow rate	tonne/hr	90.59	104.88	118.45	129.51	138.77
CO_2	mol%	2.59	2.65	2.72	2.84	2.99
H_2O		5.15	5.28	5.42	5.66	5.96
N_2		77.04	76.99	76.93	76.84	76.72
O_2		15.22	15.08	14.92	14.66	14.33
Exhaust gas temperature	℃	213	208	203	206	213
Off-design load						
High	–	Engine loads higher than the design-point load				
Low	–	Engine loads lower than the design-point load				

process design at design-point loads, column diameters and lean CO_2 loading were defined according to the design-point conditions of each capacity scenario. The design data of different capacity scenarios, used for both design-point and off-design operations, were determined, as shown in Table 4.

4.3. Off-design operations

In this study, the OCC systems were operated and analyzed under varying engine loads (Fig. 3). The off-design operations were performed by varying only the flow rate of the lean amine solvent to capture 90 % of the CO_2 emitted from different main engine loads (with varying gas flow rate and CO_2 concentration) while maintaining the design data from the corresponding capacity scenario (Table 4).

However, there is a limit to the operating range of the given absorber design from each capacity scenario due to fluid dynamic reasons [31]. The upper limit of the exhaust gas flow rate was determined to be the flow rate emitted at each design-point load. At higher engine loads than the design-point load, i.e., off-design loads (high), only the exhaust gas flow rate corresponding to the specified design-point load was fed to the absorber. The excess flow was vented from the original exhaust gas before entering the absorber, as shown in Fig. 5.

The lower limit of the exhaust gas flow rate that a column can handle was decided by the turndown ratio of a liquid distributor in a packed column, which is defined as the ratio of the maximum lean solvent flow rate to the minimum lean solvent flow rate. Thus, the exhaust gas flow rate that can be handled with the minimum lean solvent flow rate was defined as the lower limit of the exhaust gas flow rate. The typical turndown ratio ranges from 2:1 to 3:1 [36–38], which can be increased by using a dual liquid distributor [37]. However, for ship applications, it is not suitable to implement the multiple-stage distributor due to height limitations. Therefore, a turndown ratio of 2.5:1 was used in this study considering the limited height on the ship, motion dynamics, and fluid dynamic parameters [36].

The maximum lean solvent flow rate was observed at 100 % engine load for all capacity scenarios. At 100 % engine load, the exhaust gas flow rate entering the column was the same as the flow rate at each design-point load. However, the CO_2 concentration at off-design loads (high) was higher than the design-point values, requiring a larger lean solvent flow rate. After identifying the maximum lean solvent flow rate for each capacity scenario, the minimum lean solvent flow rate that could be distributed by the liquid distributor was calculated considering the turndown ratio. This minimum lean solvent flow rate was used to determine the lower limit of the exhaust gas flow rate (main engine load) entering the capture system.

Since the carbon capture process models were simulated assuming that all process models could be operated over the 25–100 % engine load range, the available operating range depending on turndown ratios could also be estimated. The OCC system designed for capacity scenario 5 required a 4:1 turndown ratio to handle the 25–100 % engine load range, while the system designed for capacity scenario 1 could cover the similar engine load range with a much lower turndown ratio (2.5:1). Thus, at low turndown ratios, larger capacity systems may have limitations in covering a low engine load range due to a narrower operating range compared to their smaller counterparts.

The corresponding engine loads of the operating ranges and

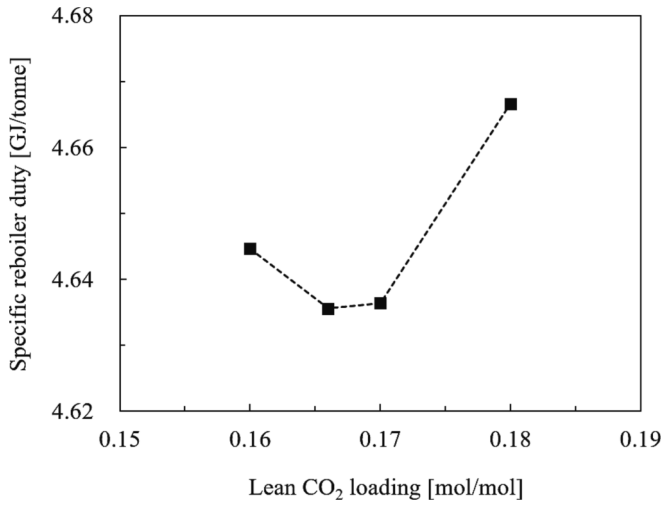

Fig. 4. Variation of specific reboiler duty with lean CO_2 loading for the design-point conditions of capacity scenario 1.

minimum engine loads for different turndown ratios are illustrated in Fig. 6. With the 2.5:1 turndown ratio, the capacity scenario 1 can be operated for the engine load ranges of 26–100 % while capacity scenario 5 can covers 41–100 % engine load. It is worth noting that when the engine load is over the design point, such as 51–100 % load for the capacity scenario 1 and 91–100 % load for capacity scenario 5, the excess flow was vented. In addition, the exhaust gas emitted below the minimum engine load, which the column could not handle, was also vented.

5. Key performance indicators

This section describes the key performance indicators (KPIs) used to evaluate the performance of OCC systems. The main engine load profile was used to integrate the off-design performance from the design-point and off-design operations for each capacity scenario to quantify the KPIs: CO_2 reduction, energy requirements, and costs for the entire voyage.

5.1. CO_2 reduction

The average CO_2 generated over a single voyage, including the CO_2 from the carbon capture systems, is calculated as:

$$\begin{aligned} \text{CO}_2\text{ generated (total) [tonne/hr]} = &\text{CO}_2\text{ generated (main engine)} \\ &+ \text{CO}_2\text{ generated (additional)} \end{aligned} \quad (1)$$

where this equation is divided into two emission sources: the CO_2 generated (main engine) by the main engine (WinGD 6X72DF) and the CO_2 generated (additional) by the generator and the MGO-fired boiler. These auxiliary units are responsible for producing electricity and additional heat for the carbon capture systems. For the term CO_2 generated (main engine), to obtain the CO_2 emissions for the entire voyage (0–100 %), the CO_2 emissions below 25 % engine load were extrapolated based on the CO_2 emission data from the 25 % to 100 % engine load range. Thus, the CO_2 generated (main engine) was evaluated for the entire voyage, while the second term, CO_2 generated (additional), was estimated only when in operation. To calculate the CO_2 generated (additional), the additional energy used by the generator and MGO-fired boiler was converted to equivalent marine gas oil (MGO) consumption. This additional fuel consumption was then multiplied by the emission factor, as shown below:

Table 4
Design data for each capacity scenario.

Category	Unit	Capacity scenario 1	Capacity scenario 2	Capacity scenario 3	Capacity scenario 4	Capacity scenario 5
Lean CO_2 loading	mol/mol	0.166	0.166	0.166	0.168	0.168
Base CO_2 capture rate	%			90		
DCC packing height	m			5		
Absorber, stripper packing height	m			10		
Water washing section packing height	m			1		
DCC diameter	m	3.72	4.01	4.28	4.50	4.69
Absorber diameter	m	3.21	3.46	3.68	3.87	4.03
Stripper diameter	m	1.22	1.32	1.42	1.50	1.58
Water washing section diameter	m	3.62	3.89	4.15	4.34	4.49
MEA concentration	wt%			30		
Exhaust gas temperature after WHRU	°C			140		
Lean solvent temperature to absorber	°C			40		
Lean-rich heat exchanger minimum temperature approach	°C			10		
Cooling water temperature	°C			30		
Absorber operating pressure	atm			1		
Stripper operating pressure	atm			2		
Captured CO_2 purity	mol%			95		

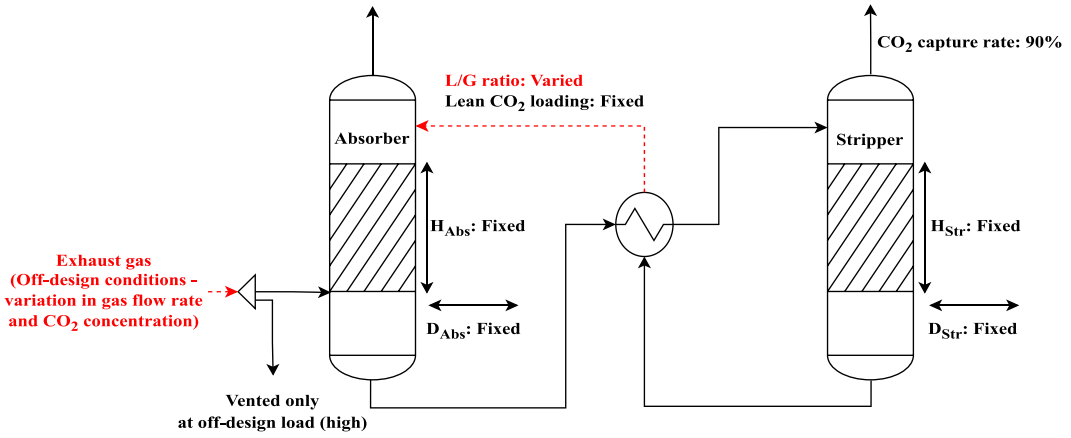

Fig. 5. Off-design operation.

$$\mathrm{CO_2\ generated\ (additional)} = \left(\mathrm{Additional\ energy\ (generator)\ [GJ_e]} \times \mathrm{SFOC} + \frac{\mathrm{Additional\ energy\ (MGO-fired\ boiler)\ [GJ_{th}]}}{\mathrm{Boiler\ efficiency} \times \mathrm{LHV_{MGO}}}\right) \times \mathrm{EF_f} \quad (2)$$

where the specific fuel oil consumption (SFOC) of the generator was obtained from the diesel engine (WinGD 5X35-B). The assumptions used to calculate the emissions are shown in Table 5.

The average CO_2 emitted after operation of the carbon capture systems is calculated as:

$$\mathrm{CO_2\ emitted\ [tonne/hr]} = \mathrm{CO_2\ generated\ (total)} - \mathrm{CO_2\ captured} \quad (3)$$

where the CO_2 captured is also obtained within the available operating range of the column.

The CO_2 avoided quantifies the actual CO_2 removal performance by introducing the capture systems. Therefore, this cumulative performance provides the CO_2 reduction for a single voyage with the OCC systems, as shown below:

$$\mathrm{CO_2\ avoided\ [tonne/hr]} = \mathrm{CO_2\ generated\ (main\ engine)} - \mathrm{CO_2\ emitted} \quad (4)$$

$$\mathrm{CO_2\ avoided\ rate\ [\%]} = \frac{\mathrm{Cumulative\ CO_2\ avoided}}{\mathrm{Cumulative\ CO_2\ generated\ (main\ engine)}} \times 100 \quad (5)$$

where the CO_2 generated (main engine) and CO_2 emitted are the CO_2 emissions of the target ship without and with the carbon capture systems, respectively.

5.2. Energy requirements

As mentioned earlier, the specific reboiler duty (SRD) was defined as the reboiler energy required to capture 1 tonne of CO_2. However, in order to reach the base carbon capture rate of 90 %, additional energy was generated in the MGO-fired boiler to supply the reboiler. Thus, the specific energy consumption (SEC) is defined as the specific additional energy for the reboiler. The cumulative SEC of CO_2 avoided quantifies net energy requirements for a single voyage with the OCC systems. It is measured by cumulative indicators of additional energy and CO_2 avoided, as shown below:

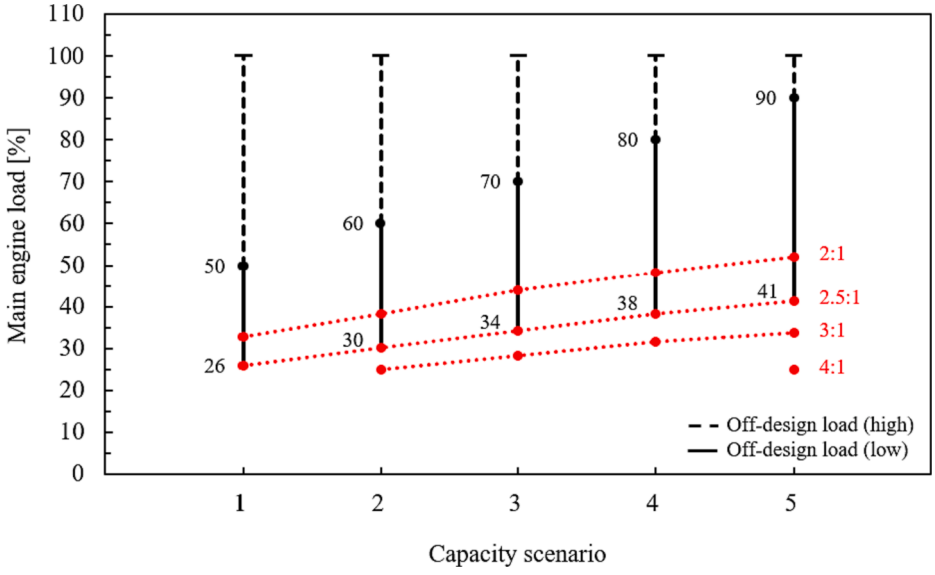

Fig. 6. Main engine load range in which the onboard carbon capture system can be operated for each capacity scenario (black circles represent the design-point load and red circles indicate minimum engine loads depending on the different turndown ratios). (For interpretation of the references to colour in this figure legend, the reader is referred to the web version of this article.)

Table 5
Assumptions used for estimating additional carbon emissions.

Category	Unit	Value
SFOC of generator	tonne/GJ	0.047
Boiler efficiency	%	85
LHV_{MGO}	GJ/tonne	42.7 [39]
Emission factor (EF_f)	$tonne_{CO_2}/tonne_{Fuel}$	3.206 [2]

$$\text{Cumulative SEC of } CO_2 \text{ avoided } [GJ_{th}/\text{tonne } CO_2 \text{avoided}] = \frac{\text{Cumulative reboiler heat duty required} - \text{Cumulative waste heat recovery}}{\text{Cumulative } CO_2 \text{ avoided}} \quad (6)$$

where the waste heat recovery is calculated cumulatively within the available operating range of the column.

5.3. Cost evaluation

The MEA-based OCC systems were evaluated on an N^{th}-of-a-kind (NOAK) basis, i.e., assuming a point in time when the technology is commercially mature [40]. The CAPEX was estimated using a bottom-up costing methodology, as shown in Fig. 7 [41,42]. Aspen Process Economic Analyzer® was used to calculate the direct costs of process equipment (e.g., packed columns, pumps, heat exchangers, blower). The total direct cost including process contingency (TDCPC) was determined using a process contingency factor, which was set to 10 % of the total direct cost (TDC). Then, the engineering, procurement, and construction cost (EPC) was calculated by summing up the TDCPC and indirect costs (set to 14 % of TDCPC). The total plant cost (TPC) was calculated by summing up the EPC and project contingencies (set to 30 % of EPC). Finally, the total capital requirement (TCR) was obtained by adding the owner costs (set to 7.5 % of TPC), interest during construction, start-up costs, and the TPC.

The OPEX is the sum of fixed OPEX (FOPEX) and variable OPEX (VOPEX). The annual FOPEX includes maintenance (set to 2.0 % of TPC), insurance and local taxes (set to 2.0 % of TPC), and labor costs. The labor cost was estimated based on the assumption of an annual salary of 60,000 € per operator and employing a total of 5 operators. The annual VOPEX is estimated taking into account the utility costs, including fuel, process water, and solvent make-up. Currently, fuel prices have risen globally due to the COVID-19 pandemic in late 2019 and the Russia-Ukraine war in February 2022. The current MGO price has significantly increased to 712 € per tonne compared to the yearly averages of 508 and 482 € per tonne observed in 2019 (pre-COVID) and 2021 (Russia-Ukraine war), respectively. In order to analyze the impact of fluctuating fuel prices on CO_2 avoidance costs, these costs were calculated based on fuel prices in 2019 (pre-COVID) and 2021 (pre-war), respectively. The estimated amount of solvent make-up was based on the amine losses due to degradation [43] and amine volatility. The utility costs are shown in Table 6.

Table 6
Costs of utilities for VOPEX [44–46].

Category	Year	Unit	Value
MGO	2019	€/tonne	508
	2021	€/tonne	482
	2023	€/tonne	712
LNG	2019	€/tonne	400 [23]
	2021	€/tonne	858
	2023	€/tonne	855
FAME	2019	€/tonne	779
	2021	€/tonne	1405
	2023	€/tonne	1270
Process water	–	€/m^3	6.65
MEA	–	€/tonne	1600

Table 7
Assumptions used for calculating carbon capture cost.

Category	Unit	Value
Economic lifetime (ship)	year	25
Annual number of round trips	–	10
Average time per round trip	hr	744.6
Operating hours	hr/year	7446
Discount rate	%	8

The CO_2 avoidance cost is the KPI used to evaluate the cost performance of MEA-based OCC systems. The CO_2 avoidance cost is calculated as [42,47]:

$$CO_2 \text{ avoidance cost } [€/\text{tonne } CO_2\text{avoided}] = \frac{\text{Annualized CAPEX} + \text{Annual FOPEX} + \text{Annual VOPEX}}{\text{Annual } CO_2 \text{ avoided}} \quad (7)$$

The annual CO_2 avoided was estimated based on the operating hours per year and the average CO_2 avoided over a single voyage. The assumptions used to calculate the CO_2 capture cost are shown in Table 7.

6. Results and discussion

6.1. Off-design performance of case study

As shown in Fig. 8 and Fig. 9, the liquid-to-gas (L/G) ratios and SRD were plotted over the available operating range for each capacity scenario. In Fig. 8, the L/G ratio increases as the design-point load increases. The high CO_2 concentration at the absorber feed stream and the high carbon capture rate contribute to a high L/G ratio [35,48]. As previously mentioned, the L/G ratios were determined to achieve the base carbon capture rate of 90 % for all operations. With the base

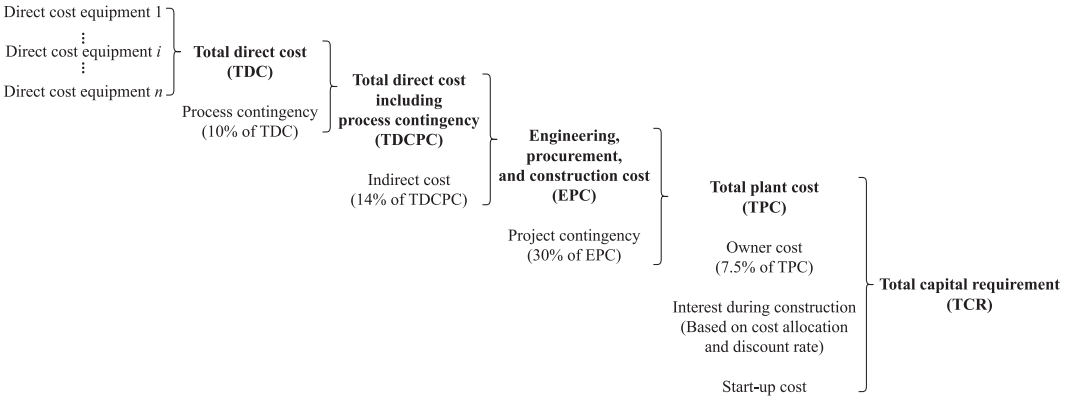

Fig. 7. Bottom-up costing methodology for CAPEX estimation [41].

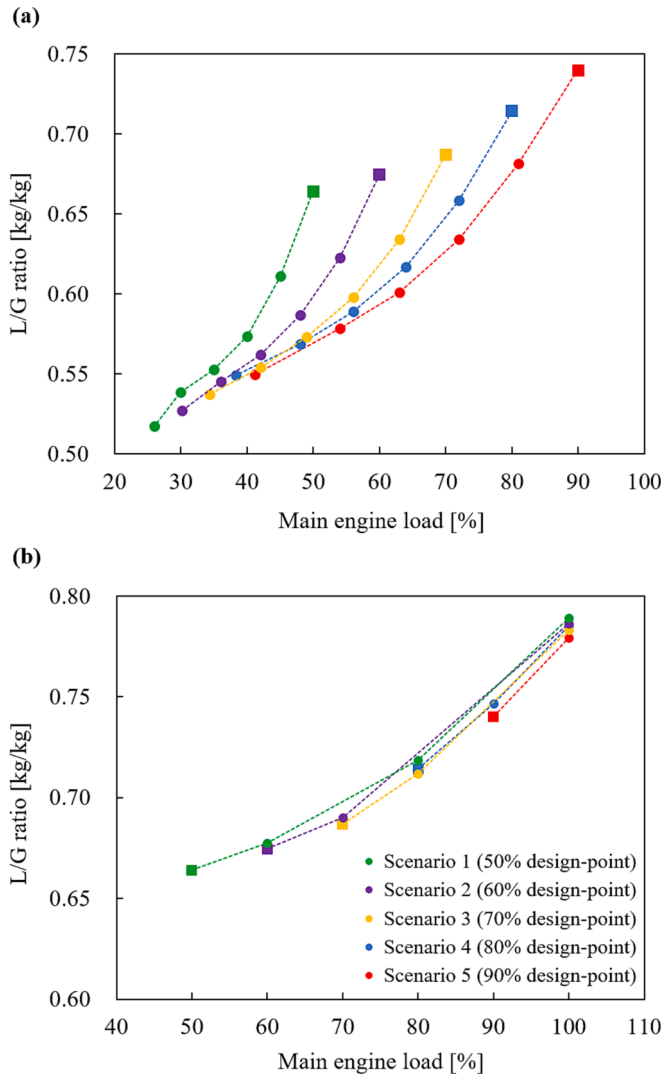

Fig. 8. Variations of L/G ratio with main engine load for different capacity scenarios: (a) L/G ratios for design-point load ranges and off-design load (low) ranges; (b) L/G ratios for off-design load (high) ranges (Squares are for design-point loads and circles are for off-design loads).

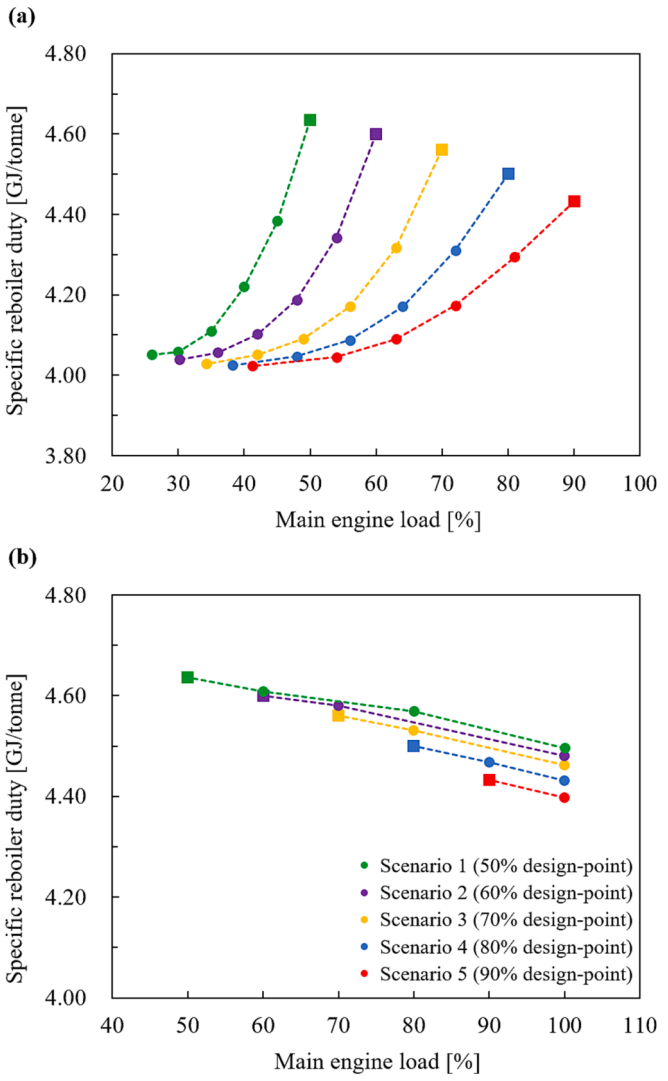

Fig. 9. Variations of specific reboiler duty with main engine load for different capacity scenarios: (a) SRD for design-point load ranges and off-design load (low) ranges; (b) SRD for off-design load (high) ranges (Squares are for design-point loads and circles are for off-design loads).

capture rate constant, an increase in engine load increased the CO_2 concentration (Fig. 2), which subsequently resulted in a higher L/G ratio (higher lean solvent flow rate). For the same reason, the L/G ratios of the off-design loads (low) for each capacity scenario are lower than the L/G ratios of their design-point loads, as shown in Fig. 8(a). Also, the L/G ratios of the off-design load (high) ranges follow the same trend as the CO_2 concentration increases, as shown in Fig. 8(b).

Fig. 9 shows that the SRD, which does not consider the waste heat recovery and the CO_2 generated (additional), gradually decreases as the design-point load increases. This trend, which is opposite to the L/G ratio results, can also be explained by the CO_2 concentration [30,31,48,49]. As discussed earlier, the specific reboiler duty comprises three components: q_{abs,co_2}, q_{sens}, and q_{vap,H_2O}. The contributions of these three components to the specific reboiler duty were estimated, as shown in Fig. 10. Comparing the energy requirements between capacity scenario 1 and capacity scenario 5, the most significant reduction is observed in the heat required to generate the stripping steam (q_{vap,H_2O}). This is because increasing the CO_2 concentration at the absorber feed stream increased both the lean and rich CO_2 loadings, as shown in Table 4 and Fig. 11, respectively. Correspondingly, the water concentration at the stripper feed stream decreased. Therefore, a relatively

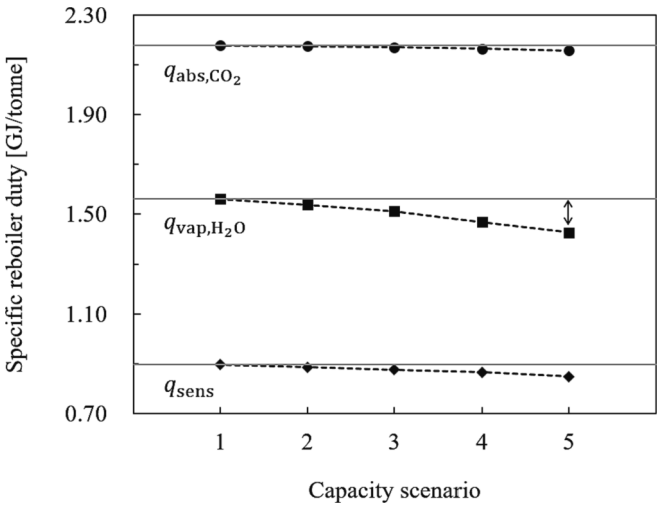

Fig. 10. Contributions to specific reboiler duty at design-point load for each capacity scenario.

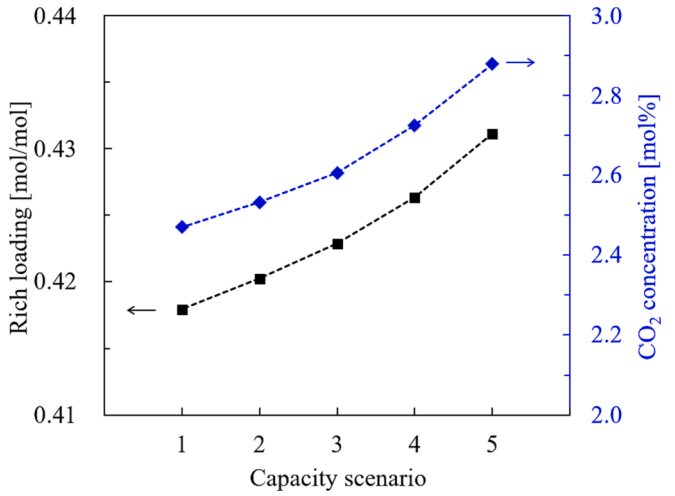

Fig. 11. Variations of rich loading with CO_2 concentration at design-point load for each capacity scenario.

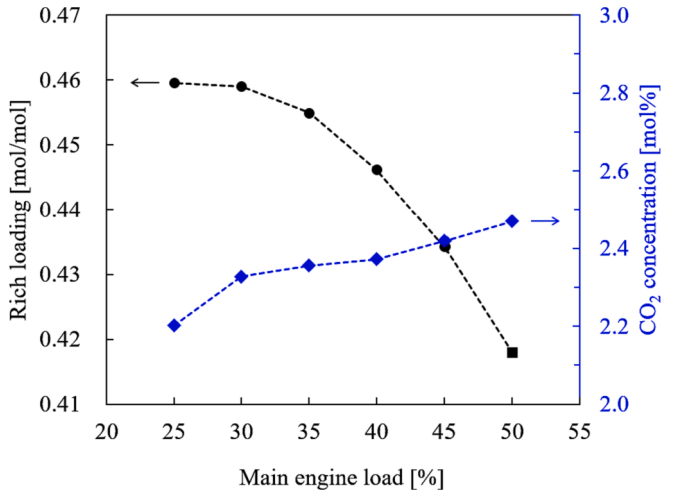

Fig. 12. Variations of rich loading and CO_2 concentration with main engine load for capacity scenario 1.

smaller amount of stripping steam was required compared to the lower design-point load. For the same reason, the SRD at the off-design loads (high) follows the same trend with increasing engine load (increasing CO_2 concentration), as shown in Fig. 9(b).

However, it is worth noting that the SRD decreases at lower loads (off-design load conditions) even though the CO_2 concentration in the exhaust gas is reduced. At the off-design loads (low), a lower flow rate of the exhaust gas enters the capture system while the column dimensions are maintained from the design values. As indicated in Fig. 12, the reduced feed flow rate leads to a relatively larger interfacial area and a higher rich CO_2 loading, resulting in a lower SRD. This trend is also observed in the pilot plant data reported by Notz et al. [31].

The off-design performance indicates that larger capacity capture systems benefit from a lower SRD. Therefore, a cumulative analysis is required to identify the actual capture potential and energy requirements of OCC systems over an entire voyage.

6.2. Cumulative performance of case study

Using the actual main engine load profile and the off-design performance, the cumulative performance for each capacity scenario for the entire voyage were quantified in terms of the following KPIs: CO_2

Table 8
Cumulative performance of the target ship with the onboard carbon capture systems over a single voyage.

Category	Unit	Target ship w/o OCC	Capacity scenario 1	Capacity scenario 2	Capacity scenario 3	Capacity scenario 4	Capacity scenario 5
Design-point load	%	–	50	60	70	80	90
CO_2 generated (total)	tonne/hr	3.56	4.44	4.48	4.46	4.40	4.39
CO_2 generated (main engine)	tonne/hr	3.56	3.56	3.56	3.56	3.56	3.56
CO_2 generated (additional)	tonne/hr	–	0.87	0.92	0.89	0.84	0.83
CO_2 captured	tonne/hr	–	2.86	3.01	2.96	2.82	2.83
CO_2 emitted	tonne/hr	3.56	1.57	1.47	1.49	1.58	1.56
CO_2 avoided	tonne/hr	–	1.99	2.09	2.07	1.99	2.00
CO_2 avoided rate	%	–	56	59	58	56	56
Cumulative SEC of CO_2 avoided	GJ_{th}/tonne	–	3.14	3.14	3.08	3.01	2.91
CO_2 avoidance cost	€/tonne	–	233	236	243	251	257
CAPEX	€/tonne	–	77	79	85	92	98
FOPEX	€/tonne	–	47	47	50	53	55
VOPEX*	€/tonne	–	110	110	108	106	104

* based on 2023 MGO price.

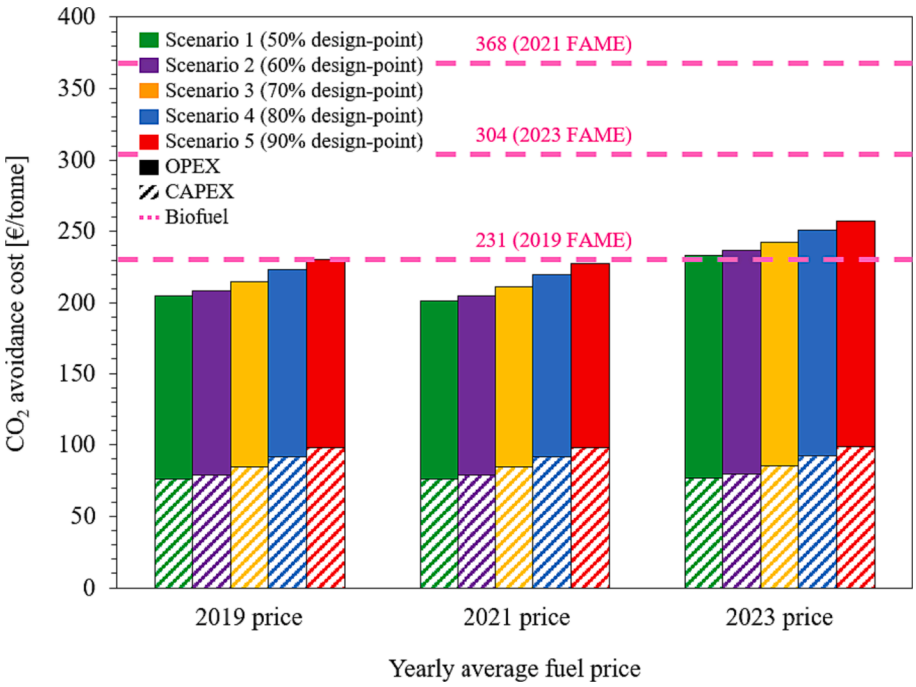

Fig. 13. CO_2 avoidance cost of the onboard carbon capture system compared to the alternative decarbonization strategy.

avoided rate, cumulative SEC, and CO_2 avoidance cost. As can be seen in Table 8, the OCC systems designed based on capacity scenarios 1–5 indicate a similar level of carbon reduction potential with a marginal deviation. Even smaller OCC systems achieve comparable emission reductions due to the low average main engine load of the target ship and the wide operating range of the absorber. However, larger OCC systems have a lower cumulative SEC than the systems based on capacity scenarios 1 and 2 due to their relatively larger interfacial area as explained in the previous section. The same trend is observed in the VOPEX, which is proportional to the energy consumption of the capture system.

However, it should be noted that the systems based on low-capacity scenarios benefit from a lower CAPEX as the capacity of the capture system decreases. Besides, the cumulative analysis shows that the CAPEX savings from a reduced capacity of the capture system outweigh the OPEX penalties, resulting in a lower CO_2 avoidance cost. For example, the system based on capacity scenario 1 has a 22 % decrease in CAPEX while VOPEX increases only by 6 % compared to the system based on capacity scenario 5, resulting in the lowest CO_2 avoidance cost (233 € per tonne). For the system based on capacity scenario 2, which has the highest CO_2 avoided rate, its compact size results in a 19 % reduction in CAPEX compared to the system based on capacity scenario 5, leading to an 8 % decrease in CO_2 avoidance cost (236 € per tonne).

The CO_2 avoidance costs estimated from this work with the two-stroke engine are found to be higher than those reported in previous studies based on four-stroke engines. The two-stroke engine has a lower CO_2 concentration and less recoverable waste heat than four-stroke engines. This results in higher fuel consumption for additional energy generation, which directly increases the OPEX of the capture system. Consequently, for OCC systems with two-stroke engines, both CAPEX and OPEX emerge as significant contributors to the total capture cost while previous studies with four-stroke engines indicate the CAPEX to be the main driver of the economic performance [19,22,23]. The importance of OPEX can also be seen in the report by OGCI and Stena Bulk [50]. They conducted a case study on a two-stroke engine with low waste heat availability that shows a similar level of avoidance costs to this study.

Thus, as one of key parameters affecting the capture cost, the fuel price (VOPEX) needs to be considered when investigating the viability of an OCC system with two-stroke engines. In particular, three different fuel prices are assumed in this work, reflecting the recent volatility of MGO prices. As can be seen in Fig. 13, the OPEX is significantly affected by fuel prices. Given that the OPEX is the major component of the total capture cost, fuel prices also become a crucial parameter. Currently, high fuel prices have resulted in increased capture costs, but if fuel prices were to return to pre-COVID levels, the CO_2 avoidance cost for the systems based on low-capacity scenarios could drop to around 200 € per tonne. Considering the potential for even greater fluctuations in fuel prices, a sensitivity analysis was conducted with a wide range of fuel prices in Appendix C.

In addition, to compare the amine-based carbon capture system with an alternative measure, CO_2 avoidance costs for the use of FAME (fatty acid methyl ester) were also calculated. FAME is the most widely used biofuel in the marine sector [51] and can be operated in existing engines without major modification. In this estimation, FAME was used until it achieved the CO_2 avoided rate of 59 %, which is the highest CO_2 avoided rate of the OCC systems in this work, and only considers the operating cost according to the FAME consumption. However, the alternative technology using FAME is not competitive with amine-based systems, as shown in Fig. 13. Based on the average annual price of the FAME in 2023, it was calculated at 304 € per tonne, which is 29 % higher than the CO_2 avoidance cost for capacity scenario 2. Even for a wide range of fuel prices (Appendix C), the OCC system is found to be economically competitive with the FAME price in 2023. From an economic perspective, this comparison shows that deployment of OCC systems is more cost-effective than the use of FAME. Therefore, OCC systems designed based on small capacity scenarios 1–2 are identified as the optimal capacities of the OCC system in terms of the CO_2 avoidance cost and the CO_2 avoided rate.

In order to generalize the optimal capacity of the OCC system identified using the actual main engine load profile, this study generated hypothetical main engine load profiles with a consistent average load of 49 % but different distributions (see Appendix B). Table 9 shows the cumulative performance calculated for their different profiles. Consistent with the findings from the actual profile, OCC systems based on capacity scenarios 1–2 are also observed as optimal capacities in most of the other generated profiles. However, while the overall trend is

Table 9
Cumulative performance for different ship profiles.

Category	Hypothetical profile 1		Hypothetical profile 2 (similar to actual profile)		Hypothetical profile 3 (similar to actual profile)	
	CO_2 avoidance cost (€/tonne)	CO_2 avoided rate (%)	CO_2 avoidance cost (€/tonne)	CO_2 avoided rate (%)	CO_2 avoidance cost (€/tonne)	CO_2 avoided rate (%)
Scenario 1	249	42	234	57	239	55
Scenario 2	266	44	237	59	245	58
Scenario 3	291	43	239	60	245	58
Scenario 4	290	46	250	56	252	56
Scenario 5	292	49	257	56	259	56

consistent, there can be a large deviation in derived cumulative performance depending on the distribution of load profiles. This is because the load profile determines two main factors. The frequency of each engine load and whether each capture system would operate within its available operating range. These factors directly affect the cumulative performance by either increasing or decreasing the carbon reduction potential of capture systems. Thus, the design approach for OCC systems should reflect variable engine loads (actual engine load profile) to avoid oversized equipment and unnecessary capital investment, and to accurately calculate cumulative performance.

7. Conclusions

This study investigated the performance of the MEA-based OCC system, reflecting an actual sailing profile. Based on the cumulative performance, this work focused on identifying the optimal capacity of the capture systems to avoid oversized equipment and unnecessary capital investment. The target vessel was an LNG-fueled container ship powered by a two-stroke low-pressure dual-fuel engine. In particular, the results of the case study indicate that OCC systems are more cost-effective than the use of FAME, even under the worst assumptions considering the characteristics of NG-fired two-stroke engine.

The smaller OCC systems can achieve a similar level of CO_2 reduction to other larger capture systems when the average engine load is low. For this load profile, smaller capture systems should vent some of the exhaust gas at high engine loads. However, by setting a lower design-point load, these systems can handle a wider load range, which offsets the CO_2 loss. This makes it possible to reduce the CO_2 avoidance cost by decreasing CAPEX while maintaining the CO_2 avoided rate. Therefore, this study provides a new approach for designing appropriately sized amine-based OCC systems on a ship where space is limited.

The CO_2 avoided rate of the OCC system is limited to below 60 % regardless of the capacity. The relatively low emission reduction potential is due to the narrow operating range of the capture system. In this study, a turndown ratio of 4:1 is required to cover the entire engine load variation. However, increasing the turndown ratio will be challenging under shipboard conditions. Therefore, determining a feasible turndown ratio is expected to be essential to improve the capture potential and the economic viability of amine-based OCC systems.

Another key aspect in designing and evaluating OCC systems is the engine load profile of a voyage. The engine load profile will vary depending on various factors. Thus, in this work, both design-point and off-design performance is quantified in advance so that any sailing profiles can be applied to evaluate the cumulative KPIs. This methodology is also expected to offer a suitable engine load profile when OCC systems are implemented on a target vessel, increasing the emission reduction potential.

This work initially focused on the optimal capacity of an OCC system to minimize capital investment. However, both CAPEX and OPEX are found to be equally important to the CO_2 avoidance cost. In particular, the low temperature exhaust gas from two-stroke engines results in a relatively small amount of waste heat to be recovered, increasing fuel consumption for additional heat generation onboard. Therefore, further efforts are necessary to reduce the OPEX of capture systems, such as optimizing the onboard heat exchange network and increasing the exhaust gas temperature with minimal engine efficiency loss.

CRediT authorship contribution statement

Juyoung Oh: Conceptualization, Data curation, Formal analysis, Methodology, Validation, Visualization, Writing – original draft, Writing – review & editing, Investigation. **Donghoi Kim:** Conceptualization, Investigation, Methodology, Project administration, Writing – review & editing, Funding acquisition, Resources, Supervision. **Simon Roussanaly:** Conceptualization, Funding acquisition, Investigation, Methodology, Project administration, Writing – review & editing,

Resources. **Rahul Anantharaman:** Conceptualization, Investigation, Methodology, Writing – review & editing, Funding acquisition, Project administration, Resources. **Youngsub Lim:** Conceptualization, Funding acquisition, Investigation, Methodology, Project administration, Resources, Supervision, Writing – review & editing.

Declaration of competing interest

The authors declare that they have no known competing financial interests or personal relationships that could have appeared to influence the work reported in this paper.

Data availability

Data will be made available on request.

Acknowledgments

This work was supported by Korea Institute for Advancement of Technology (KIAT) grant funded by the Korea Government (MOTIE) (P0017304, Human Resource Development Program for Industrial Innovation) and the Korea Research Institute of Ships and Ocean engineering, grant from Endowment Project of "Technology Development of Onboard Carbon Capture and Storage System and Pilot Test" funded by Ministry of Oceans and Fisheries (PES4750). This work was also supported by the KSP project CCShip under the MAROFF program of the Research Council of Norway (RCN project number 320260). The authors would like to acknowledge the following partners for their support: the NCCS Research Centre and its partners (Aker Carbon Capture, Allton, Ansaldo Energia, Baker Hughes, CoorsTek Membrane Sciences, Equinor, Fortum Oslo Varme, Gassco, KROHNE, Larvik Shipping, Lundin Norway, Norcem, Norwegian Oil and Gas, Quad Geometrics, Stratum Reservoir, Total, Vår Energi, Wintershall DEA), Calix Limited, Klaveness, Wärtsilä, and the Research Council of Norway. The Research Institute of Marine Systems Engineering and Institute of Engineering Research at Seoul National University provided research facilities for this work.

Appendix A. Model validation and process design

A.1 Model validation

The validation was performed by comparing the key simulation results, such as lean and rich CO_2 loadings, CO_2 capture rate, and reboiler heat duty, with the pilot plant data (Table A.1) and then adjusting key factors (Table A.2). The validated rate-based model yielded simulation results that are similar to the experimental data, as shown in Table A.1. The correlations and tuning factors used for the validated rate-based model are summarized in Table A.2.

Table A.1
Comparison of key simulation results with pilot plant data

Category	Unit	Pilot plant data [31]	Validated model	Absolute percentage error (%)
Flue gas	kg/h	72.1		–
CO_2	mol%	3.5		–
H_2O		7.6		–
N_2		75.8		–
O_2		13.1		–
Lean loading	mol CO_2/mol MEA	0.232	0.232	0.1
Rich loading		0.31	0.313	1.3
CO_2 capture rate	%	84.6	84.9	0.3
Reboiler heat duty	kW	6.7	7.36	10

Table A.2
Specifications of the validated rate-based model.

Category	Value
Calculation type	Rate-based calculation
Packing material	Mellapak 250Y [31,35]
Reaction condition factor	0.7
Film discretization ratio	5
Flow model	VPlug
Interfacial area factor	1.2
Mass transfer coefficient method	Brf-85 [52]
Heat transfer coefficient method	Chilton and Colburn [53]
Interfacial area method	Brf-85 [52]
Holdup method	Brf-92 [54]
Film resistance	Discrxn for liquid film; Film for vapor film

A.2 Process design

The scale-up model of OCC systems consists of three main columns: a direct contact cooler (DCC), an absorber including a water washing section, and a stripper. The DCC, installed upstream of the absorber, cools the exhaust gas that has passed through a WHRU because the CO_2 absorption in an aqueous MEA solution is more favorable at lower exhaust gas temperatures. It can also reduce the volume flow rate of the exhaust gas, which affects the size of the columns. The exhaust gas, cooled to about 45 ℃ via the DCC, enters the absorber and the CO_2 in the exhaust gas is absorbed into the lean (regenerated) amine solvent. The scrubbed gas from the top of the absorber is washed through the water washing section to minimize amine losses

before being vented as clean gas. The rich amine solvent, which leaves the bottom of the absorber, passes through a lean-rich heat exchanger and enters the stripper. Then, the CO_2 in the rich amine solvent is desorbed by the heat input through a reboiler in the stripper. Finally, the captured CO_2 is obtained from the top of the stripper while the hot regenerated solvent from the bottom of the stripper passes through the lean-rich heat exchanger and circulates back to the absorber.

Appendix B. Hypothetical profiles

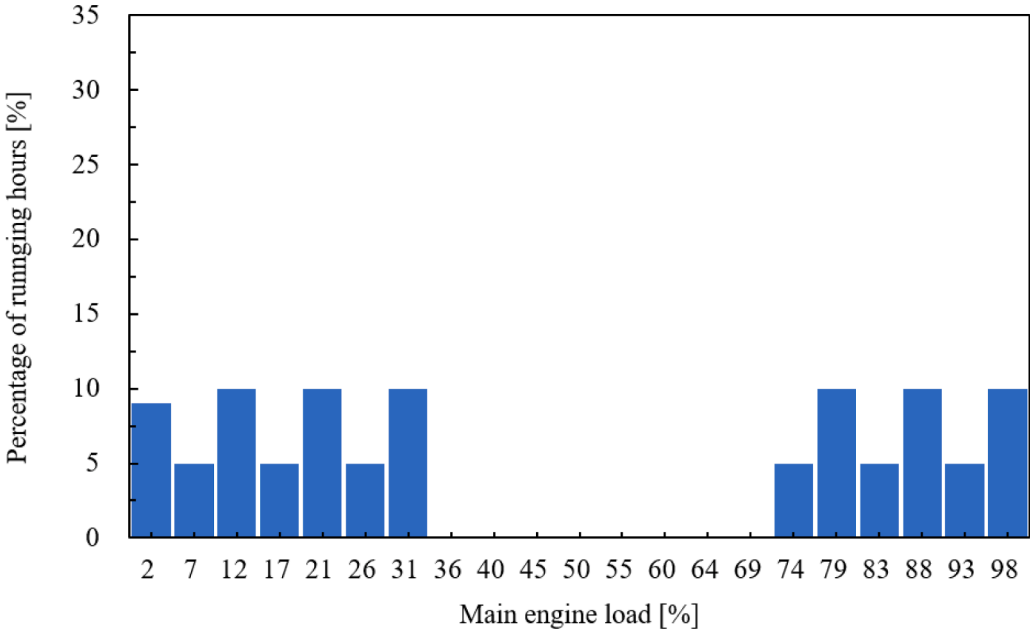

Fig. B.1. Hypothetical profile 1.

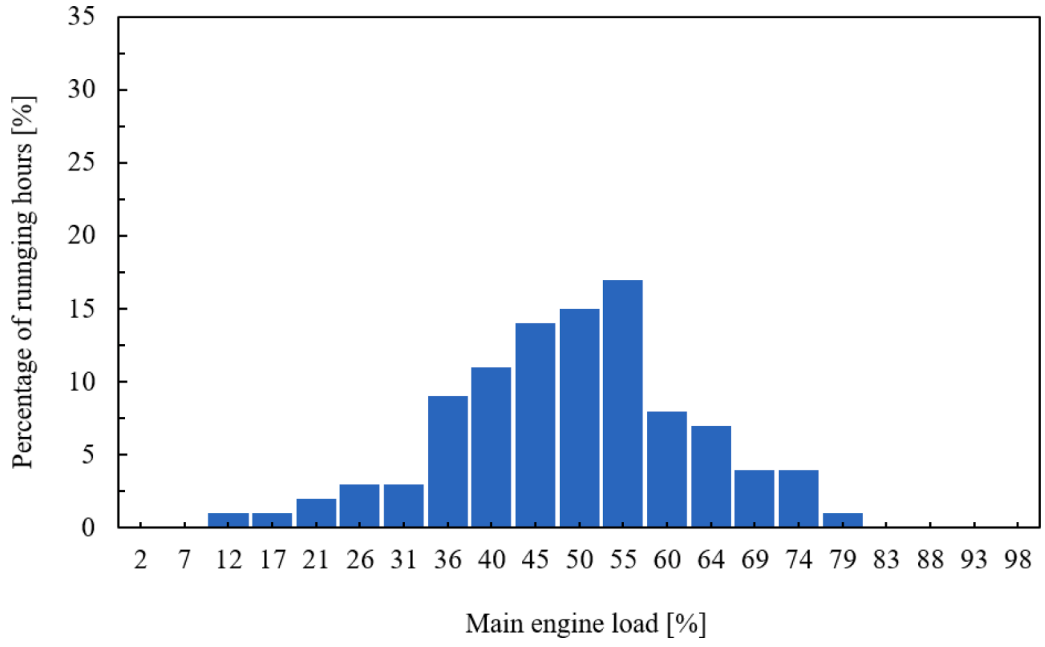

Fig. B.2. Hypothetical profile 2.

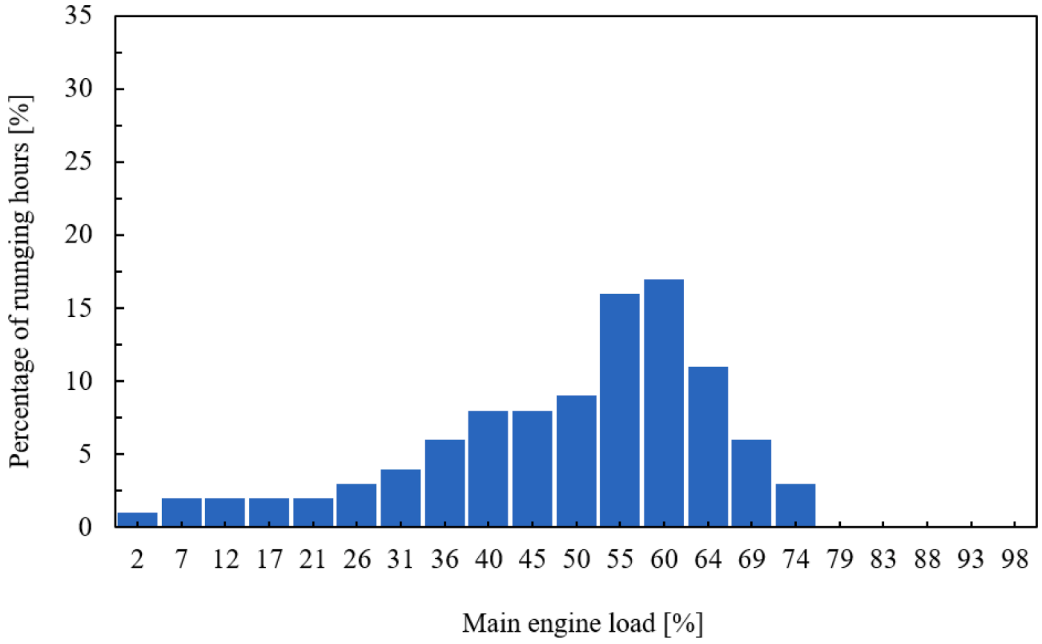

Fig. B.3. Hypothetical profile 3.

Appendix C. Sensitivity analysis

The analysis evaluated the impact of fluctuations in fuel prices on CO_2 avoidance costs, with MGO prices ranging from 400 to 1000 € per tonne, as shown in Fig. C.1. It is worth noting that even with MGO prices increasing to 1000 € per tonne, the CO_2 avoidance cost for using FAME based on its 2023 fuel price remains higher than those of the OCC systems.

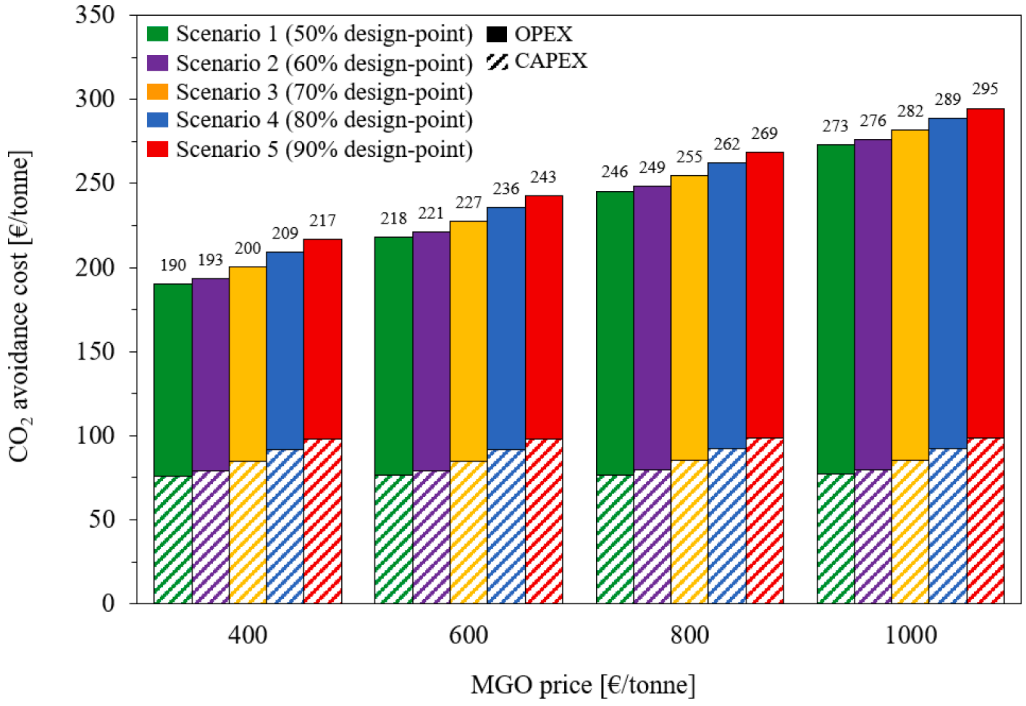

Fig. C.1. Impact of different MGO prices on CO_2 avoidance costs.

References

[1] Scripps Institution of Oceanography, The Keeling Curve, 2022. https://keelingcurve.ucsd.edu/ (accessed June 7, 2022).
[2] IMO, Fourth IMO GHG Study 2020, 2021.
[3] IMO, Resolution MEPC.304(72); Initial IMO strategy on reduction of GHG emissions from ships, 2018.
[4] IMO, 2021 Amendments to the Annex of the Protocol of 1997 to Amend the International Convention for the Prevention of Pollution from Ships, 1973, as Modified by the Protocol of 1978 Relating Thereto 2021 Revised MARPOL Annex VI (Resolution MEPC.328(76)), 2021.
[5] IMO, Report of the Marine Environment Protection Committee on its Seventy-Sixth Session, 2021.
[6] IMO, Resolution MEPC.377(80); 2023 IMO strategy on reduction of GHG emissions from ships, 2023.
[7] E.A. Bouman, E. Lindstad, A.I. Rialland, A.H. Strømman, State-of-the-art technologies, measures, and potential for reducing GHG emissions from shipping – A review, Transp Res D Transp Environ 52 (2017) 408–421, https://doi.org/10.1016/j.trd.2017.03.022.
[8] J. Jung, Y. Seo, Onboard CO2 Capture Process Design using Rigorous Rate-based Model, Journal of Ocean Engineering and Technology 36 (2022) 168–180, https://doi.org/10.26748/ksoe.2022.006.
[9] F. Ueckerdt, P.C. Verpoort, R. Anantharaman, C. Bauer, F. Beck, T. Longden, S. Roussanaly, On the cost competitiveness of blue and green hydrogen, Joule (2024), https://doi.org/10.1016/j.joule.2023.12.004.
[10] J.-Y. Park, J.-Y. Jung, Y.-T. Seo, Investigation of Applying Technical Measures for Improving Energy Efficiency Design Index (EEDI) for KCS and KVLCC2, Journal of Ocean Engineering and Technology 37 (2023) 58–67, https://doi.org/10.26748/KSOE.2023.001.
[11] M. Steyn, J. Oglesby, G. Turan, A. Zapantis, R. Gebremedhin, N. Al Amer, I. Havercroft, R. Ivory-Moore, X. Yang, M. Abu Zahra, E. Pinto, D. Rassool, E. Williams, C. Consoli, J. Minervini, Global Status of CCS 2022, 2022. https://status22.globalccsinstitute.com/wp-content/uploads/2022/12/Global-Status-of-CCS-2022_Download_1222.pdf (accessed February 16, 2023).
[12] Korean Register, IMO News Final MEPC 80, 2023.
[13] J. Oh, R. Anantharaman, U. Zahid, P. Lee, Y. Lim, Process design of onboard membrane carbon capture and liquefaction systems for LNG-fueled ships, Sep. Purif. Technol. 282 (2022) 120052, https://doi.org/10.1016/j.seppur.2021.120052.
[14] H.F. Svendsen, E.T. Hessen, T. Mejdell, Carbon dioxide capture by absorption, challenges and possibilities, Chem. Eng. J. 171 (2011) 718–724, https://doi.org/10.1016/j.cej.2011.01.014.
[15] M.G. Plaza, F. Rubiera, Development of carbon-based vacuum, temperature and concentration swing adsorption post-combustion CO2 capture processes, Chem. Eng. J. 375 (2019), https://doi.org/10.1016/j.cej.2019.122002.
[16] B. Adhikari, C.J. Orme, C. Stetson, J.R. Klaehn, Techno-economic analysis of carbon dioxide capture from low concentration sources using membranes, Chem. Eng. J. 474 (2023), https://doi.org/10.1016/j.cej.2023.145876.
[17] Y. Kim, J. Lee, H. Cho, J. Kim, Novel cryogenic carbon dioxide capture and storage process using LNG cold energy in a natural gas combined cycle power plant, Chem. Eng. J. 456 (2023), https://doi.org/10.1016/j.cej.2022.140980.
[18] X. Luo, M. Wang, Study of solvent-based carbon capture for cargo ships through process modelling and simulation, Appl. Energy 195 (2017) 402–413, https://doi.org/10.1016/j.apenergy.2017.03.027.
[19] M. Feenstra, J. Monteiro, J.T. van den Akker, M.R.M. Abu-Zahra, E. Gilling, E. Goetheer, Ship-based carbon capture onboard of diesel or LNG-fuelled ships, Int. J. Greenhouse Gas Control 85 (2019) 1–10, https://doi.org/10.1016/j.ijggc.2019.03.008.
[20] S. Lee, S. Yoo, H. Park, J. Ahn, D. Chang, Novel methodology for EEDI calculation considering onboard carbon capture and storage system, Int. J. Greenhouse Gas Control 105 (2021) 103241, https://doi.org/10.1016/j.ijggc.2020.103241.
[21] N.V.D. Long, D.Y. Lee, C. Kwag, Y.M. Lee, S.W. Lee, V. Hessel, M. Lee, Improvement of marine carbon capture onboard diesel fueled ships, Chem. Eng. Process. - Process Intesif. 168 (2021), https://doi.org/10.1016/j.cep.2021.108535.
[22] A. Awoyomi, K. Patchigolla, E.J. Anthony, Process and Economic Evaluation of an Onboard Capture System for LNG-Fueled CO2 Carriers, Ind. Eng. Chem. Res. 59 (2020) 6951–6960, https://doi.org/10.1021/acs.iecr.9b04659.
[23] J.A. Ros, E. Skylogianni, V. Doedée, J.T. van den Akker, A.W. Vredeveldt, M.J. G. Linders, E.L.V. Goetheer, J.-G.-M.-S. Monteiro, Advancements in ship-based carbon capture technology on board of LNG-fuelled ships, Int. J. Greenhouse Gas Control 114 (2022), https://doi.org/10.1016/j.ijggc.2021.103575.
[24] UNCTAD, REVIEW OF MARITIME TRANSPORT 2022., 2023.
[25] C. Ji, S. Yuan, M. Huffman, M.M. El-Halwagi, Q. Wang, Post-combustion carbon capture for tank to propeller via process modeling and simulation, J. CO2 Util. 51 (2021), https://doi.org/10.1016/j.jcou.2021.101655.
[26] M. Stec, A. Tatarczuk, T. Iluk, M. Szul, Reducing the energy efficiency design index for ships through a post-combustion carbon capture process, Int. J. Greenhouse Gas Control 108 (2021), https://doi.org/10.1016/j.ijggc.2021.103333.
[27] A. Einbu, T. Pettersen, J. Morud, A. Tobiesen, C.K. Jayarathna, R. Skagestad, G. Nysæther, Energy assessments of onboard CO2 capture from ship engines by MEA-based post combustion capture system with flue gas heat integration, Int. J. Greenhouse Gas Control 113 (2022), https://doi.org/10.1016/j.ijggc.2021.103526.
[28] IMO, Third IMO GHG Study 2014, 2015.
[29] Wärtsilä, WSD80 3800 Container Feeder DATASHEET, 2016. https://cdn.wartsila.com/docs/default-source/product-files/sd/merchant/feeder/wsd80-3800-container-feeder-ship-design-o-data-sheet.pdf (accessed July 28, 2022).
[30] J. Husebye, A.L. Brunsvold, S. Roussanaly, X. Zhang, Techno economic evaluation of amine based CO2 capture: impact of CO2 concentration and steam supply, Energy Procedia 23 (2012) 381–390, https://doi.org/10.1016/j.egypro.2012.06.053.
[31] R. Notz, H.P. Mangalapally, H. Hasse, Post combustion CO2 capture by reactive absorption: Pilot plant description and results of systematic studies with MEA, Int. J. Greenhouse Gas Control 6 (2012) 84–112, https://doi.org/10.1016/j.ijggc.2011.11.004.
[32] AspenTech, ENRTL-RK Rate-Based Model of the CO2 Capture Process by MEA using Aspen Plus - Version 10.0, Bedford, MA, USA, 2008. http://www.aspentech.com.
[33] H.Z. Kister, J.R. Haas, D.R. Hart, D.R. Gill, Distillation Design, McGraw-Hill, New York, 1992.
[34] M. Biermann, F. Normann, F. Johnsson, R. Skagestad, Partial Carbon Capture by Absorption Cycle for Reduced Specific Capture Cost, Ind. Eng. Chem. Res. 57 (2018) 15411–15422, https://doi.org/10.1021/acs.iecr.8b02074.
[35] E.O. Agbonghae, K.J. Hughes, D.B. Ingham, L. Ma, M. Pourkashanian, Optimal Process Design of Commercial-Scale Amine-Based CO2 Capture Plants, Ind. Eng. Chem. Res. 53 (2014) 14815–14829, https://doi.org/10.1021/ie5023767.
[36] Koch-Glitsch, PACKED TOWER Internals, 2020. https://koch-glitsch.com/technical-documents/brochures/packed-tower-internals (accessed April 8, 2023).
[37] H.Z. Kister, Distillation Operation, McGraw-Hill, 1990.
[38] Sulzer Chemtech, Internals for packed columns, 2010.
[39] WinGD, Marine Installation Manual X72DF-1.1, 2021. https://www.wingd.com/en/search/?q=marine%20installation%20manual (accessed January 4, 2024).
[40] S. Roussanaly, E.S. Rubin, M. Van der Spek, G. Booras, N. Berghout, T. Fout, M. Garcia, S. Gardarsdottir, V. Nair Kuncheekanna, M. Matuszewski, S. Mccoy, J. Morgan, S. Mohd Nazir, A. Ramirez, Towards improved guidelines for cost evaluation of carbon capture and storage-a white paper, 2021.
[41] S.G. Subraveti, S. Roussanaly, R. Anantharaman, L. Riboldi, A. Rajendran, How much can novel solid sorbents reduce the cost of post-combustion CO2 capture? A techno-economic investigation on the cost limits of pressure–vacuum swing adsorption, Appl. Energy 306 (2022), https://doi.org/10.1016/j.apenergy.2021.117955.
[42] S. Roussanaly, N. Berghout, T. Fout, M. Garcia, S. Gardarsdottir, S.M. Nazir, A. Ramirez, E.S. Rubin, Towards improved cost evaluation of Carbon Capture and Storage from industry, Int. J. Greenhouse Gas Control 106 (2021), https://doi.org/10.1016/j.ijggc.2021.103263.
[43] M. Campbell, S. Akhter, A. Knarvik, Z. Muhammad, A. Wakaa, CESAR1 Solvent degradation and thermal reclaiming results from TCM testing, in: Proceedings of the 16th Greenhouse Gas Control Technologies Conference (GHGT-16), 2022, https://doi.org/10.2139/ssrn.4286150.
[44] Bunker Index, Bunker Index: Rotterdam, Netherlands, 2023. https://bunkerindex.com/index.php (accessed June 13, 2023).
[45] S.O. Gardarsdottir, E. De Lena, M. Romano, S. Roussanaly, M. Voldsund, J.F. Pérez-Calvo, D. Berstad, C. Fu, R. Anantharaman, D. Sutter, M. Gazzani, M. Mazzotti, G. Cinti, Comparison of Technologies for CO2 Capture from Cement Production—Part 2: Cost Analysis, Energies (basel) 12 (2019), https://doi.org/10.3390/en12030542.
[46] Neste, Biodiesel prices (SME & FAME), 2023. https://www.neste.com/investors/market-data/biodiesel-prices-sme-fame#f29d80dc (accessed June 13, 2023).
[47] S. Roussanaly, Calculating CO 2 avoidance costs of Carbon Capture and Storage from industry, Carbon Manag 10 (2019) 105–112, https://doi.org/10.1080/17583004.2018.1553435.
[48] R. Notz, I. Tönnies, H.P. Mangalapally, S. Hoch, H. Hasse, A short-cut method for assessing absorbents for post-combustion carbon dioxide capture, Int. J. Greenhouse Gas Control 5 (2011) 413–421, https://doi.org/10.1016/j.ijggc.2010.03.008.
[49] S. Freguia, G.T. Rochelle, Modeling of CO2 Capture by Aqueous Monoethanolamine, AIChE J 49 (2003) 1676–1686, https://doi.org/10.1002/aic.690490708.
[50] OGCI and Stena Bulk, Is carbon capture on ships feasible?, 2021. https://www.ogci.com/wp-content/uploads/2021/11/OGCI_STENA_MCC_November_2021.pdf (accessed February 16, 2023).
[51] DNV, Use of biofuels in shipping, 2023. https://www.dnv.com/news/use-of-biofuels-in-shipping-240298 (accessed June 30, 2023).
[52] J.L. Bravo, J.A. Rocha, J.R. Fair, Mass transfer in gauze packings, Hydrocarb. Process. 64 (1985) 91–95.
[53] R. Taylor, R. Krishna, Multicomponent mass transfer, John Wiley & Sons, New York, 1993.
[54] J.L. Bravo, J.A. Rocha, J.R. Fair, A comprehensive model for the performance of columns containing structured packings, Inst. Chem. Eng. Symp. Ser. 129 (1992) A439.